Acta Neuropathol (2000) 100:347–355

REGULAR PAPER

Yoshihito Tanoi · Riki Okeda · Herbert Budka

Binswanger's encephalopathy: serial sections and morphometry of the cerebral arteries

Received: 15 November 1999 / Revised, accepted: 28 December 1999

Abstract To identify arterial changes that are characteristic of Binswanger's encephalopathy (BE), we analyzed cerebral subarachnoid and medullary arteries of seven BE autopsy specimens by reconstruction of stained serial sections. We also noted the frequency of intimal fibrosis with or without atheroma of the subarachnoid arteries, and determined the medial thickness of the subarachnoid and medullary arteries. The results for the BE specimens were compared with those of six hypertensive brain hemorrhage (HH) specimens and six normotensive (NT) specimens from patients without cerebral abnormalities. In medullary arteries of BE in comparison with HH, we observed nonspecific but significantly more widespread intimal fibrosis with or without atheroma, as well as segmental loss of the medial smooth muscle cells (SMCs), which was sometimes associated with intimal plasma exudation or microaneurysm. A few medullary arteries in BE were completely occluded by fibrous connective tissue. Intimal fibrosis of the subarachnoid arteries was significantly more widespread in BE than in HH and NT. The media of the subarachnoid and medullary arteries was significantly thicker in BE and HH than in NT, and tended to be thicker in BE than in HH. In NT specimens the medullay arteries tended to be thinner in medial thickness than the subarachnoid arteries. These findings suggest that dysfunction of blood flow regulation due to increased arterial stiffness caused by hypertension-induced intimal fibrosis and loss of medial SMCs is an essential mechanism resulting in diffuse myelin loss of the cerebral white matter in BE, whereas luminal stenosis or occlusion and adventitial fibrosis are secondary. Moreover, selective and severe involvement of the cerebral medullary arteries compared with the subarachnoid arteries may be explained by the following two factors, (1) that many medullary arteries have normally dilated sigments, and (2) that their media is thinner compared with that of the subarachnoid arteries of the corresponding diameter.

Key words Binswanger's encephalopathy · Hypertension · Hypertensive brain hemorrhage · Morphometry · Medial thickness of artery

Y. Tanoi · R. Okeda (✉)
Department of Neuropathology, Medical Research Institute, Tokyo Medical and Dental University, No. 1-5-45, Yushima, Bunkyo-ku, Tokyo, Japan

H. Budka
Institute of Neurology, University of Vienna, Allgemeines Krankenhaus 4J, Währinger Gürtel 18-20, 1097 Vienna, Austria

Introduction

Neuropathology of Binswanger's encephalopathy (BE) is characterized by diffuse myelin loss and atrophy of the cerebral white matter, sparing the cortex and subcortical U-fibers, in addition to prominent sclerotic and hypertensive changes of the cerebral arteries, which are often associated with lacunae and/or hemorrhage of the parenchyma of the central nervous system (CNS). Hence, BE is sometimes called "subcortical arteriosclerotic encephalopathy" [8]. Although it is generally accepted that the arterial changes of BE are caused by hypertension [6, 7], the nature, distribution and relationship between such arterial changes and the mechanism of selective involvement of the cerebral white matter are not known [1]. It has been proposed that severe arterial stenosis or occlusion is responsible for the myelin loss [9]. Alternatively, perivascular fibrosis or mural fibrohyalinosis of the small arteries and arterioles in the cerebral white matter may be an essential feature of BE [2].

The aim of the present study was to identify the vascular changes that characterize BE, to determine whether these changes are caused by hypertension, and, if so, to determine the difference between BE and hypertensive brain hemorrhage (HH) in term of the vascular changes.

Therefore, we compared the cerebral medullary arteries of the frontal lobe in seven autopsy specimens of BE, six of HH and in six specimens from normotensive (NT)

Table 1 Cases of BE, HH and NT (*BE* Binswanger's encephalopathy, *HH* hypertensive brain hemorrhage, *NT* normotensive cases, *Au* Austria, *Jn* Japan, *y* year, *d* day, *bl* bleeding, *ALS* Amyotrophic lateral sclerosis, *PSP* progressive supranuclear palsy)

Case	Age (year)	Gender (Nation)	Clinical diagnosis	Disease duration	Heart weight (g)
BE					
1	65	M (Au)	BE	15 y	?
2	66	F (Au)	Vascular encephalopathy	7 y	?
3	61	F (Au)	BE	4 y	?
4	59	M (Au)	BE	1 y	?
5	59	F (Au)	BE	?	?
6	60	F (Au)	Vascular encephalopathy	?	?
7	52	F (Jn)	PSP	8 y	740
Mean 60.2 ± 4.6					
HH					
1	55	F (Jn)	Hypertensive cerebral bl.	5 d	420
2	66	M (Jn)	Hypertensive putaminal bl.	1 d	420
3	46	M (Jn)	Hypertensive putaminal bl.	3 d	?
4	59	M (Jn)	Hypertensive pontine bl.	17 d	460
5	71	F (Jn)	Thalamic bleeding	1 d	380
6	69	M (Au)	Hypertensive angiopathy	1 d	?
Mean 61 ± 9.5					420.0 ± 32.6*
NT					
1	60	F (Jn)	ALS		250
2	74	F (Jn)	ALS		290
3	60	M (Jn)	Hepatoma		275
4	66	M (Jn)	ALS		300
5	64	F (Jn)	Liver cirrhosis, hepatoma Pulmonary tuberculosis		270
6	68	F (Jn)	Pulmonary tuberculosis		300
Mean 65.3 ± 5.3					280.8 ± 19.6

* Significantly ($P < 0.002$) larger than that of NT

patients. The brain tissues were examined histologically and the sections of the cerebral medullary arteries penetrating from the cortical surface to the distal level in the deep white matter of the cerebral medullary arteries were reconstructed from serial sections. We also examined the extent of intimal fibrosis of the subarachnoid arteries, and the medial thickness of the cerebral subarachnoid and medullary arteries as an indicator of the degree of hypertension in those arteries.

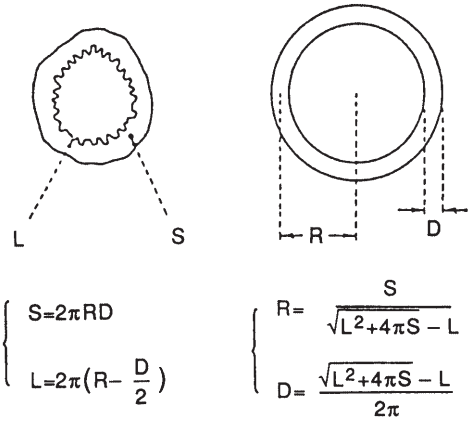

Fig. 1 Furuyama's method for measuring the arterial radius *(R)* and medial thickness *(D)* of a distended arteries (*L* length, *S* cut surface area)

Tissues and methods

Nowadays early detection and management of hypertension is common. Thus, calssical BE, that is, onset between 40 and 50 years of age and death before the age of 70, is now very rare. Therefore, the seven specimens of BE that we studied were collected over several years 1965–1971 at the University Vienna (six cases), and in Japan (one case in 1979). We also examined age-matched control autopsy specimens from six patients with HH and from six NT patients without involvement of the cerebrum. Five of the HH patients were Japanese and the other was European. The six NT patients had been diagnosed with sporadic amyotrophic lateral sclerosis without cerebral involvement (three cases), hepatoma (two cases) and pulmonary tuberculosis (one case). The mean heart weight of the NT patients was 280 g (range 250–300 g). The patients' age and gender and the duration of the clinical course are shown in Table 1. The features of the frontal lobe seen on gross examination of the BE and HH speciments are shown in Fig. 3 A, B (Klüver-Barrera stain).

Fig. 2 Reconstructed medullary arteries of BE (**A**) and HH (**B**). ▶ The internal elastic membrane of each artery is indicated by a *black line*, intimal fibrosis and atheroma are indicated by a *green zone*, defects of the medial smooth muscle layer are indicated by *red lines* (circumferential and continuous defects are marked by a *solid line*, and discontinuous defects by a *dotted line*), plasma exudation is indicated in *orange*, and adventitial fibrosis is indicated by a *blue line* (a *bold line* indicates that the fibrosis was thicker than the media). Microaneurysms are marked as "*A*". *Asterisks* indicate "L"-shaped medullary artery (*BE* Binswanger's encephalopathy, *HH* hypertensive brain hemorrhage)

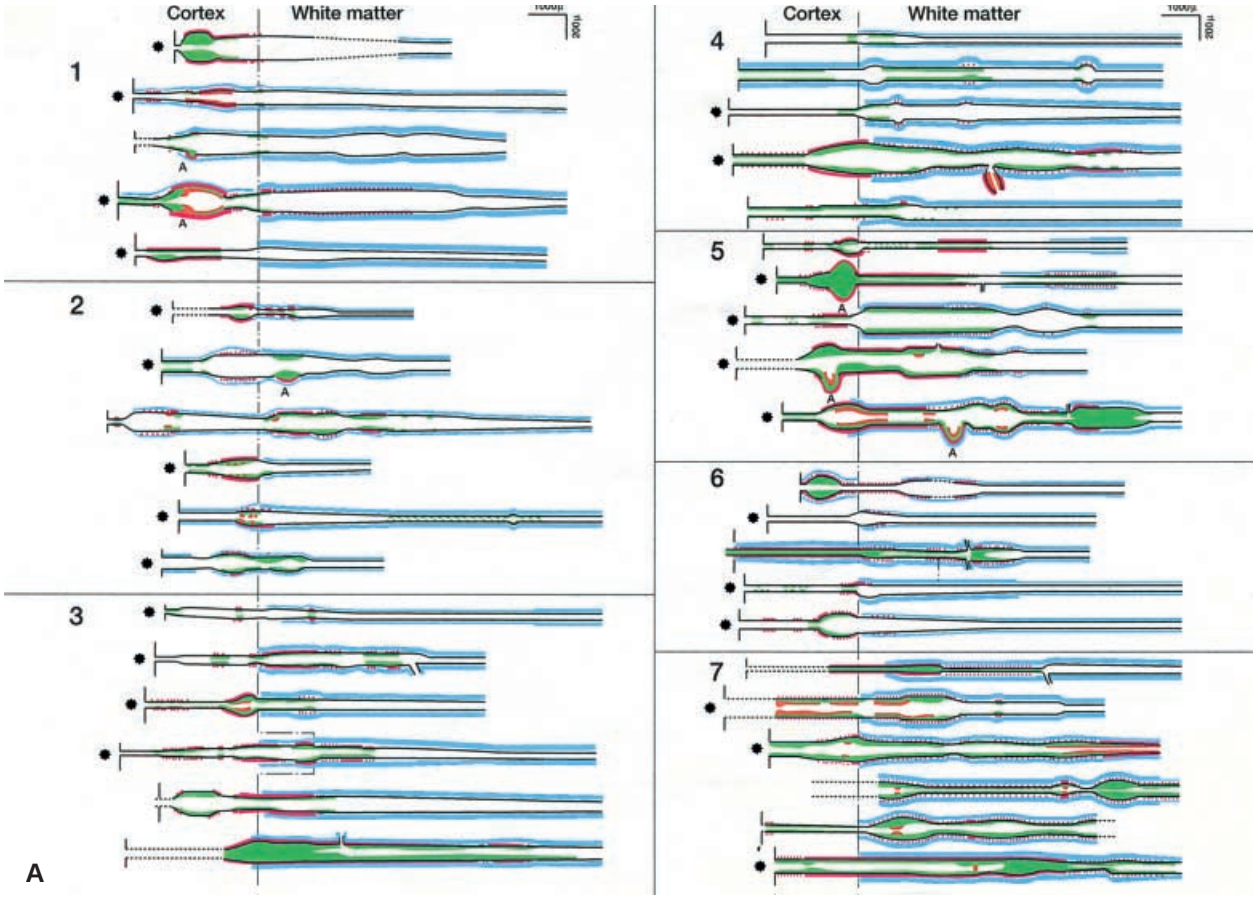
Cortex
White matter
1000µ
200µ
1
2
3
4
5
6
7
A

A

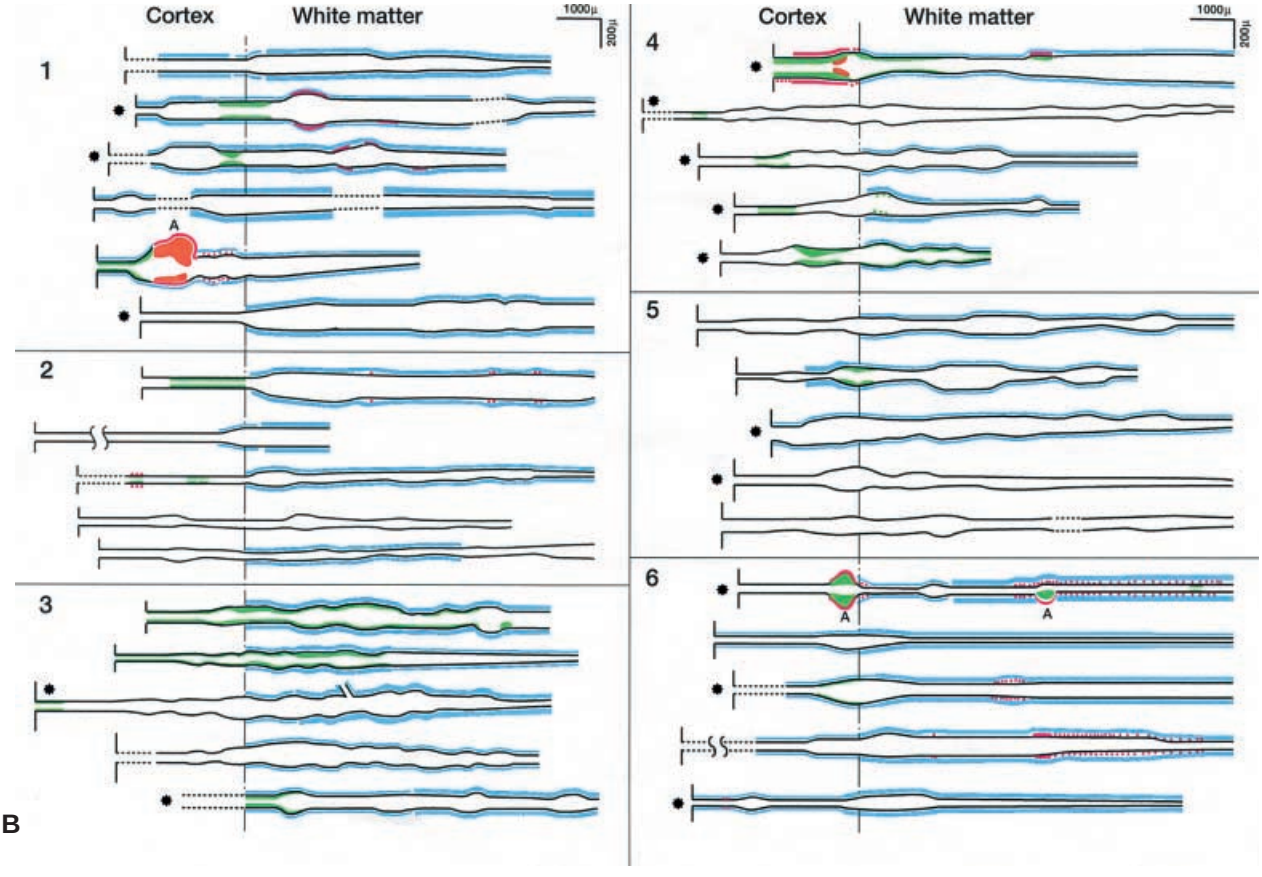
Cortex
White matter
1000µ
200µ
1
2
3
4
5
6
A

B

Nature and distribution of histological changes

For all of the BE and HH specimens and two of six NT specimens, a block of the frontal lobe from the corpus callosum to the medial portion of the middle frontal gyrus was cut from a formalin-fixed coronal section at the level of the caudate head. Each of these blocks was embedded in paraffin and about 700–1000 serial slices (5 μm thick) were cut. Every fifth slice was stained by Elastica-Masson staining. All of the medullary arteries identified in these slices were traced individually on transparent films from the penetrating site at the cortical surface to the distal portion in the deep white matter at a maximum depth of 12 000 μm from the corticomedullary junction. Then, for each of the traced arteries, we examined the internal elastic membrane, and noted any intimal fibrosis and atheroma, loss of medial smooth muscle cells (SMCs), plasma exudation, microaneurysm and adventitial fibrosis. These changes were compared between the BE, HH and NT groups. Short medullary arteries distributing to U-fibers were excluded from the analysis. Loss of SMCs was ascertained by immunohistochemical staining using monoclonal mouse antibody to human alpha-smooth muscle actin (DAKO, Denmark) in some slides. Small arteries were differentiated from venules by presence of the internal elastic membrane and when these have medial loss and obscure internal elastic membrane, by continuity to the proximal segment of the arteries in the serial sections. BE was differentiated from amyloid angiopathy and from cerebral autosomal dominant arteriopathy with subcortical infarcts and leukoencephalopathy (CADASIL) with diffuse myelin loss of the cerebral white matter by the absence of Congo-red-positive and periodic acid-Schiff (PAS)-positive deposits in the arteries. For the other four NT specimens, 10–20 frontal sections (5 μm thick) positioned 50–100 μm apart were collected and stained with Elastica-Masson stain.

Extent of intimal fibrosis with or without atheroma of the subarachnoid arteries

The only histological change seen in the subarachnoid arteries was intimal fibrosis with or without atheroma except for a few instances of microaneurysm, so we analyzed the frequency of intimal fibrosis in the sectioned arteries: we examined the internal elastic membrane and intimal fibrosis of all artery cross-sections in five to ten tissue sections, selected at random. Each artery was classified by its R: $R < 25$ μm, $25 < R < 50$ μm, $50 < R < 100$ μm and $R > 100$ μm. The frequency of intimal fibrosis-positive arteries was counted for each case and the extent of intimal fibrosis was graded: no intimal fibrosis, fibrosis extending over one-half or less of the circumfrerence, and fibrosis over more than one-half of the circumference. The numbers of arteries counted per case were 144–565, 38–130, 20–72 and 21–41, for the four groups of R, respectively.

The frequency (%) of each level of fibrosis was averaged for BE and then compared to the averages for HH using Student's *t*-test. Prominent stenosis (over 50% reduction in the lumen) was scarce in the subarachnoid arteries in BE and in HH, and complete occlusion was absent, so the grade of stenosis was not analyzed.

Medial thickness

The thickness of the medial layer of individual arteries in serial sections was analyzed morphometrically according to Furuyama's method [4] (Fig. 1), because the medial thickness reflects the degree of blood pressure burden; briefly, L of the internal elastic membrane and S of the medial layer of nearly right-angle sectioned arteries were measured using a morphometric apparatus (Cosmozone R500, Nikon Corp., Tokyo, Japan). Arteries showing medial fibrosis or loss of SMCs, which were seen only in the medullary arteries of BE and HH specimens, were not included. From these values of length (L) and cut surface area (S), the midwall radius (R) and medial thickness (D) of the artery in a distended state were calculated. The number of subarachnoid and medullary arteries measured per case was 35–92 and 33–69, respectively. When plotted on double-logarithmic coordinates there was a linear relationship between R and D (that is, $\log D = \log a + b \cdot \log R$, and therefore, $D = b \cdot D^a$; a and b are coefficients), so the coefficients of the regression line and a 95% confidence range of the mean value of D (D95%) were calculated using the following statistical formula:

$$D95\% = D \pm t_{0.05} \cdot s\sqrt{\frac{1}{n} + \frac{(R - \bar{R})^2}{s_{xx}}}$$

where $t_{0.05}$ is the critical value for *t* statistic (0.05 percentile point of the *t* distribution), s is the sample standard deviation (SD) about the regression line, *n* is the sample number, and s_{xx} is the sum of squares of deviation of R. The coefficient of the slope of the regression line was almost 1.0 for $R > 100$ μm, so D/R was almost independent of R for those arteries (Fig. 5 A). Therefore, the D/R values of those arteries were calculated and averaged for each case. The number of arteries examined per case was 6–18. These values were then averaged for BE (seven cases), HH (six cases) and NT (six cases), respectively, and compared using Student's *t*-test. The coefficient of the slope of the regression line for arteries with $R < 100$ μm was clearly lower than 1.0, so D was a non-linear function of R (Fig. 5 A), and therefore, we calculated D for R = 10, 20, 30, 40, 50, 60, 70, and 90 μm from the regression line separately for each case. These values of D and the coefficients of regression lines were compared using Student's *t*-test between BE, HH and NT.

Fig. 3 A–I Macroscopic and histological findings of BE, HH and NT. **A** Klüver-Barrera-stained sections from six cases of BE *(upper half)* and HH *(lower half)*. **B** A section from a Japanese case of BE. All cases of BE showed not only diffuse myelin loss, but also severe atrophy of the corpus callosum. **C** Severe intimal fibrosis with continuous loss of SMCs of the media in the intracortical segment of a medullary artery. BE case 1. **D** Dilatation with loss of medial SMCs and a microaneurysm *(arrow)* in an intracortical artery segment. BE case 2. **E** Intimal fibrosis with continuous and circumferential loss of medial SMCs in a dilated subcortical segment. BE case 6. **F** Partial loss of medial SMCs in a dilated subcortical segment. HH case 1. **G** Complete occlusion by fibrous connective tissue associated with diffuse loss of medial SMCs and waving of the internal elastic membrane in an intracortical segment. BE case 3. **H** A dilated and meandering medullary artery in the subcortical white matter with markedly thickened media and adventitia. Note the absence of fibrosis and deposition of extracellular matrix. BE case 1. **I** Marked dilatation of an intracortical segment of a medullary artery from an NT patient. Note the well-preserved medial SMCs. NT case 5 (*SMCs* smooth muscle cells, *NT* nomotensive). **C–E**, **G–I** Elastica-Masson staining. **F** Immunostaining for smooth muscle actin. C, D, F, G, I × 140; E × 280; H × 70 ▶

Fig. 5 A–D Morphometrical findings of the medial thickness of the subarachnoid and medullary arteries in BE, HH and NT. **A** Relation between R *(x axis)* and the D/R value *(y axis)* in NT case 2. Generally the D/R values of large arteries ($R > 100$ μm) were constant, but those of smaller arteries ($R < 100$ μm) showed a non-linear relation to R. **B** Regression lines between R and D of the subarachnoid *(red)* and medullary *(green)* arteries, with the 95% confidence range *dotted lines)* of the mean value of D (D95%) in NT (case 5). The regression line of the subarachnoid artery with the D95% lines is above that of the medullary artery, indicating that the subarachnoid artery has a significantly thicker media than the medullary artery. **C, D** Regression lines between R and D of the subarachnoid and medullary arteries in BE, HH and NT (*R* radius, *D* medial thickness)

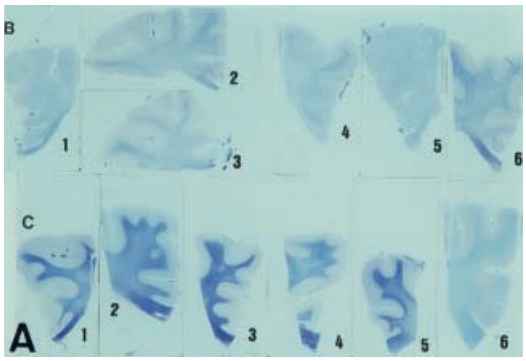

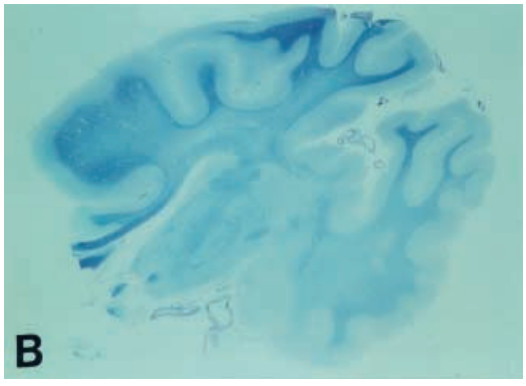

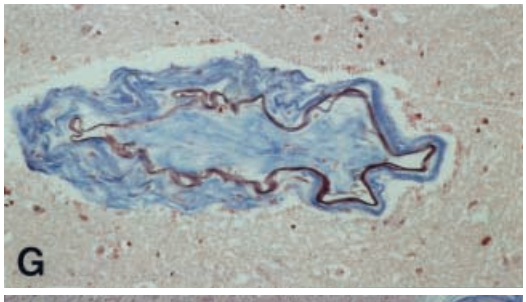

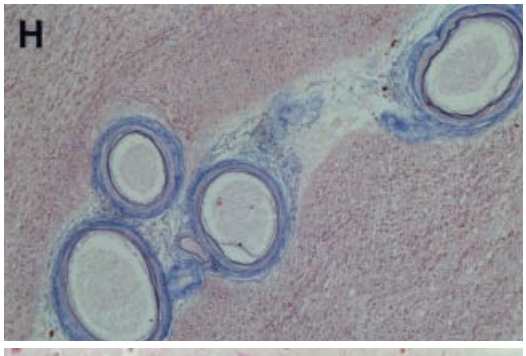

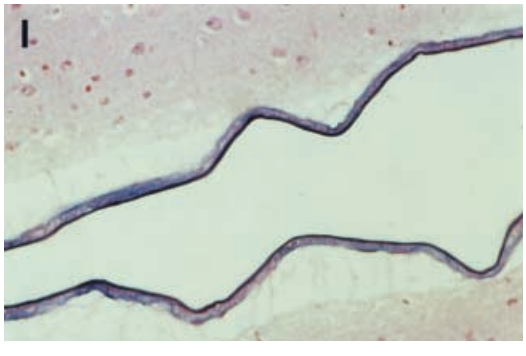

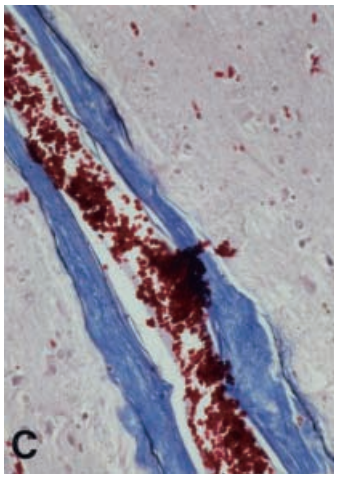

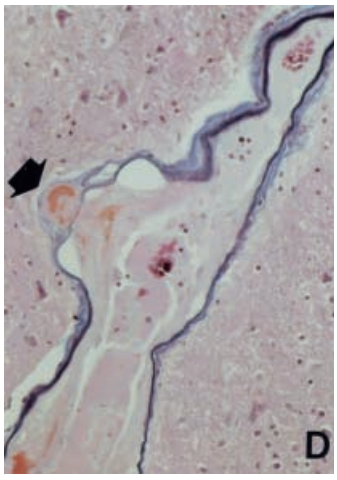

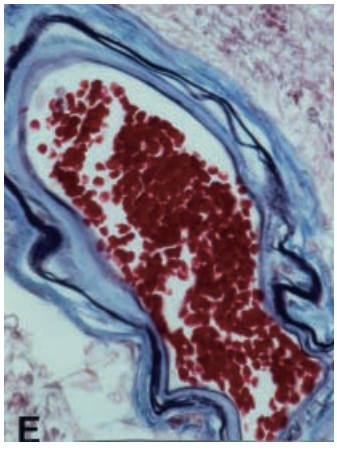

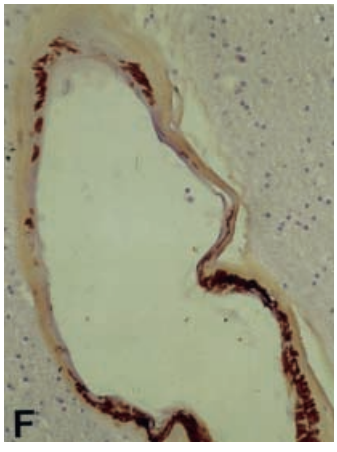

Fig. 3 A–I

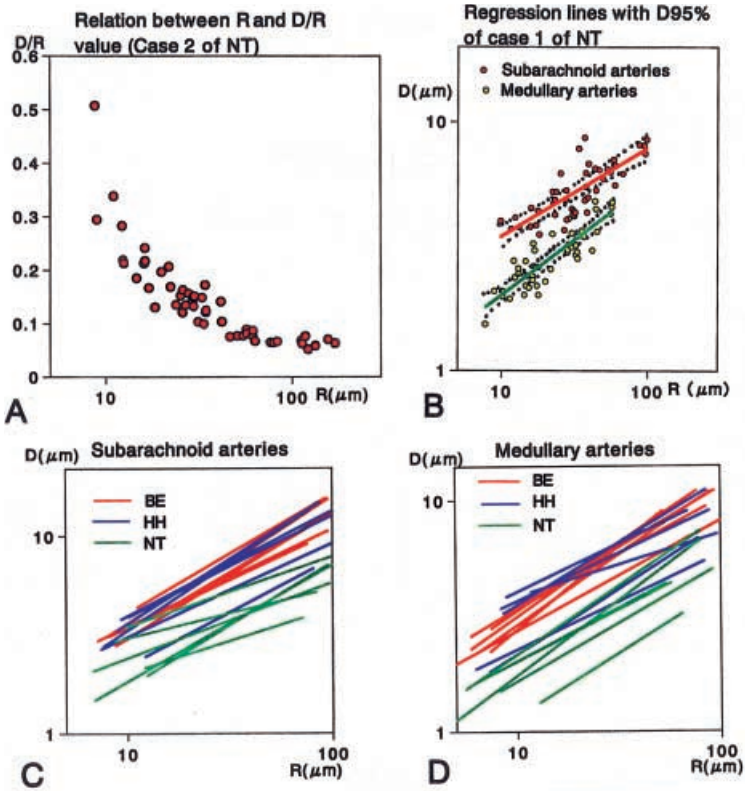

Fig. 5 A–D

Results

Reconstruction of the cerebral medullary arteries

Figure 2A, B shows the results for BE and HH. For each specimen, long sections of five to seven medullary arteries were observed. The total length of arteries examined per specimen was not significantly different between the BE (5.5 cm) and HH (5.4 cm) groups. Most of the medullary arteries in the deep white matter that was more than 8500 μm away from the corticomedullary junction were not diseased except for only segmental luminal dilatation and/or adventitial fibrosis.

Arterial dilatation, which was observed in all specimens, began in the cortex, but it was more prominent in the subcortical white matter of both of BE and HH specimens. Some of the dilated regions were associated with atherosclerosis or loss of medial SMCs, but dilatation without atheroma or other mural abnormalities was common in BE and HH. The mean maximal dilatation values expressed as the ratio of the diameters of the dilated region and the orifice at the cortical surface for the BE and HH groups were 3.2 (range 2–5) and 2.6 (range 2–4) in the cortex, and 3.4 (range 2–6) and 3.0 (range 2–4) in the white matter, respectively. There was no significant difference in the maximal dilatation between the two groups. Moreover, dilatation without mural abnormality of the medullary arteries was seen frequently in the subcortical white matter of NT specimens (Fig. 3I): the diameter of the dilated artery was twice that of the orifice in 10 of 13 medullary arteries, and it was ten times greater in two medullary arteries. Therefore, we concluded that dilatation without mural abnormality was not a pathological feature of BE and HH.

The second prominent change we observed was intimal fibrosis with or without atheroma (green zone in Fig. 2), which was present mainly in the intracortical and subcortical regions. The frequency and extent of arterial intimal fibrosis were significantly greater in BE than in HH for both the cortex and white matter. Although complete segmental occlusion of long length of artery by fibrous connective tissue (Fig. 3G) was seen in six arteries in three of seven cases of BE, stenosis of more than 80% of the original lumen was rare in BE, so we concluded that severe stenosis or occlusion is not an essential feature of BE. In the distal regions of these occluded vessels tiny lacunae were always present. Complete occlusion was never seen in HH. In NT cases intimal fibrosis and atheroma were absent.

The third important change was the continuous or discontinuous loss of SMCs in the media (Fig. 2), which we observed mainly in the intracortical and subcortical regions. SMC loss occurred not only in segments showing intimal fibrosis (Fig. 3C), but also in segments showing dilatation with or without intimal fibrosis (Fig. 3D, E). The frequency and extent of SMC loss in the cortex and white matter were significantly greater in BE than in HH. Areas of SMC loss were usually fibrotic (Fig. 3E), but in the dilated segments fibrosis was inconstant (Fig. 3D). SMC loss was frequently associated with intimal plasma or fibrin exudation (Fig. 2) and microaneurysm (Figs. 2, 3D) in both BE and HH, and these changes tended to be more frequent in BE than in HH. Microaneurysm was seen in both in the intracortical and subcortical segments, and prefered, although statistically not significant, to the medullary arteries having "L"-shaped bend at the subcortical segment (5 microaneurysms in 25 L-shaped medullary arteries) rather than ones showing straight course

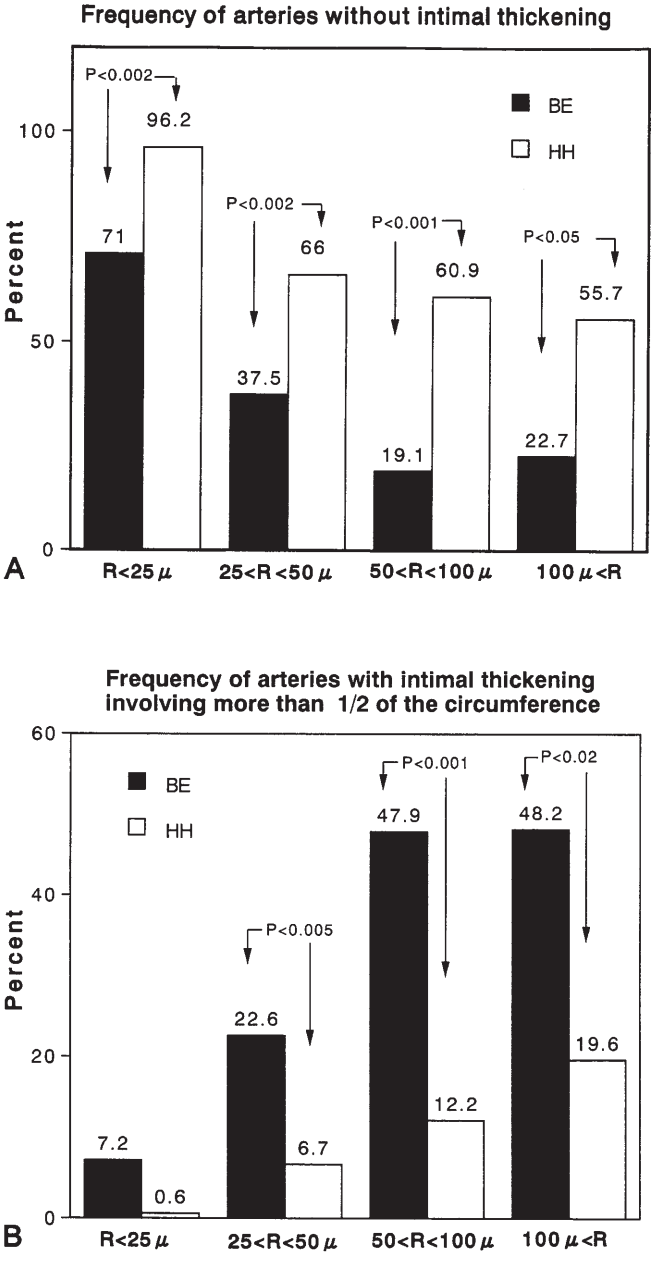

Fig. 4A, B Comparison of the frequency (%) of intimal fibrosis in subarachnoid arteries between BE and HH. **A** Frequency of arteries without intimal fibrosis. **B** Frequency of arteries with intimal fibrosis involving more than one-half of the circumference

Table 2 Coefficients of regression lines between R and D of subarachnoid arteries (mean ± SD) (*R* radius, *D* medial thickness)

	R < 100 μm		R > 100 μm	
	Slope	Constant	Slope	Constant
BE (*n* = 7)	0.59 ± 0.08*	–0.05 ± 0.09	0.93 ± 0.07	–0.68 ± 0.18
HH (*n* = 6)	0.57 ± 0.08	–0.05 ± 0.12	0.94 ± 0.08	–0.75 ± 0.27
NT (*n* = 6)	0.42 ± 0.15	–0.05 ± 0.26	1.06 ± 0.22	–1.28 ± 0.50

* Significantly ($P < 0.05$) larger than NT

Table 3 Coefficient of regression lines between R and D of medullary arteries

	Slope	Constant
BE (*n* = 7)	0.56 ± 0.09*	–0.08 ± 0.11**
HH (*n* = 6)	0.43 ± 0.10	0.07 ± 0.19***
NT (*n* = 6)	0.53 ± 0.08	–0.28 ± 0.14

* Significantly ($P < 0.05$) larger than HH, ** significantly ($P < 0.02$) larger than NT, *** significantly ($P < 0.005$) larger than NT

(1 microaneurysm in 11 straight medullary arteries). In the NT specimens, loss of medial SMCs was never seen.

The fourth change, adventitial fibrosis (Figs. 2; 3E, H) was seen frequently. It was continuous in long sections of artery and was more frequent in the white matter than in the cortex in all three groups. Severe fibrosis, fibrous material thicker than the media, tended to be more frequent in BE (22 of 38 medullary arteries) than in HH (16 of 31 medullary arteries), but the difference was not significant. It was seen in 6 of 13 medullary arteries in the NT specimens.

Frequency of intimal fibrosis with or without atheroma

As seen in Fig. 4B, the frequency of arteries without intimal abnormalities was significantly lower in BE than that of HH. Conversely, arteries with intimal thickening involving more than one-half of the circumference were more frequent in BE than in HH, and this difference was significant except for the group of R < 50 μm arteries. Therefore, we concluded that the subarachnoid arteries are involved more extensively in BE than in HH. In both BE and HH, larger arteries showed intimal fibrosis more often than smaller arteries. In the NT specimens, intimal fibrosis was rare.

Medial thickness

As shown in Fig. 5C, D, the regression lines of all cases of BE were above those of the NT specimens and did not overlap them, whereas those of the HH specimens were scattered between and overlapped those of the cases of BE and NT. Tables 2 and 3 shows the means and SDs of the regression line coefficients for the subarachnoid arteries and separately for the medullary arteries; the mean of slope of the coefficient of the medullary arteries of the BE group was significantly ($P < 0.05$) greater than that of the HH group. The slope of the coefficient of the subarachnoid arteries of the BE group was significantly ($P < 0.05$) greater than that of the NT group, and the constant coefficient of the medullary arteries was significantly greater in each of the BE ($P < 0.02$) and HH (< 0.005) groups than that of the NT group. Tables 4–6 show the mean medial thickness (D) at R = 10, 20, 30, 40, 50, 70, and 90 μm of the subarachnoid and medullary arteries and the D/R value for the subarachnoidal arteries with R > 100 μm. The subarachnoid and medullary arteries of the BE and HH groups had significantly thicker media, except at R = 10 μm, than the arteries of the NT group. The medial thickness of the subarachnoid arteries with R = 10–90 μm was always greater for the BE specimens than for the HH specimens, but the difference was not significant (Table 4). The medullary arteries also showed a similar trend, except that at R = 90 μm the media of the BE specimens were significantly ($P < 0.05$) thicker than those of the HH specimens (Table 5). The D/R value at R > 100 μm was significantly greater for BE and HH specimens than for

Table 4 Medial thickness of each group of the subarachnoid arteries

	10 μm	20	30	40	50	70	90
BE (*n* = 7)	3.5 ± 0.3**	5.2 ± 0.5*	6.6 ± 0.8*	7.9 ± 1.0*	9.0 ± 1.3*	11.0 ± 1.8*	12.8 ± 2.2*
HH (*n* = 6)	3.3 ± 0.3	4.9 ± 1.0##	6.2 ± 1.3*	7.4 ± 1.7#	8.5 ± 2.1#	10.4 ± 2.9#	12.1 ± 3.6#
NT (*n* = 6)	2.4 ± 0.7	3.2 ± 0.7	3.8 ± 0.8	4.3 ± 0.8	4.7 ± 0.9	5.4 ± 1.0	6.0 ± 1.3

* $P < 0.001$, ** $P < 0.02$, # $P < 0.005$, ## $P < 0.01$

Table 5 Medial thickness of each group of the medullary arteries

	R = 10 μm	20	30	40	50	70	90
BE (*n* = 7)	3.1 ± 0.3*	4.6 ± 0.4*	5.8 ± 0.6*	6.8 ± 0.8*	7.8 ± 1.0*	9.4 ± 1.4*	10.9 ± 1.8*††
HH (*n* = 6)	3.1 ± 0.8#	4.2 ± 0.1#	5.1 ± 1.2##	5.8 ± 1.3##	6.4 ± 1.5**	7.5 ± 1.8†	8.3 ± 2.1†
NT (*n* = 6)	1.8 ± 0.4	2.6 ± 0.5	3.2 ± 0.7	3.7 ± 0.8	4.2 ± 1.0	5.1 ± 1.2	5.8 ± 1.5

* $P < 0.001$, ** $P < 0.02$, # $P < 0.005$, ## $P < 0.01$, † $P < 0.05$, thicker than NT, †† $P < 0.05$, thicker than HH

Table 6 D/R value of arteries of R > 100 μm of each group

	BE (n = 7)	HH (n = 6)	NT (n = 6)
D/R value	0.15 ± 0.02*	0.14 ± 0.02**	0.07 ± 0.01

* $P < 0.005$, ** $P < 0.001$, as compared with NT

NT specimens, but was similar for the BE and HH specimens (Table 6). The D/R value of the medullary arteries with R > 100 μm was not examined because large arteries were scarce in the cerebral white matter.

Histologically, the medial thickening seen in the BE and HH specimens had the appearance of medial hypertrophy, because fibrosis and massive deposits of extracellular ground substance were not present in the measured arteries (Fig. 3H).

In the NT group, the media of the subarachnoid arteries of about R < 100 μm were always thicker than the media of the medullary arteries (Tables 4–6), but this difference was not statistically significant. However, when the D values of individual case of the NT group were compared between the subarachnoid and medullary arteries, the 95% confidence range of the mean value of D (D95%) of the subarachnoid arteries was separately above that of the medullary arteries in the region of R < 24–90 μm in five of six cases (Fig. 5B).

Discussion

Extent and nature of observed histopathological and morphometrical changes were similar in specimens from BE patients of Japan and Austria, so race differences do not seem to play a role in this disease.

The present histopathological and morphometrical observations support the theory that pathological changes of the subarachnoid and medullary arteries in BE are caused by hypertension, and that intimal fibrosis with or without atheroma, and loss of medial SMCs from the cerebral medullary arteries are characteristic of BE. Therefore, these changes in the medullary arteries, which were seen mainly in the intracortical and subcortical segments (that is, in the proximal segments of these arteries) rather than in the deeper white matter, induce arterial stiffness and disturb the blood flow to the cerebral white matter. It is well known that in amyloid angiopathy and CADASIL arterial damage, such as amyloid deposition or loss of SMCs with PAS-positive deposits, occur in the proximal portion (mainly intracortical region) of the medullary arteries in addition to damage to the small subarachnoid arteries and induce diffuse myelin loss of the white matter.

Severe and widespread adventitial fibrosis and occlusion were more frequently observed in the BE than in the HH, but the difference was not statistically significant. These changes, therefore, probably resulted from the increased burden of high blood pressure and flow. Furuta et al. [2] reported that in BE, cerebral medullary arteries with an external diameter under 100 μm present significantly thicker walls due to fibrohyaline thickening compared with age-matched non-neuropsychiatric autopsy cases. However, the medullary arteries that Furuta et al. [2] examined belonged to more distal segments, and the wall thickening observed included medial changes, such as the medial hypertrophy and fibrosis of the previously hypertrophied media, in addition to the adventitial fibrosis, and comparison with hypertensives without dementia was not performed in their observation. Therefore, it is not conclusive that fibrohyaline thickening of the wall of the small medullary arteries is essential for BE.

By what mechanism are these severe changes induced selectively in the cerebral medullary arteries in BE? Morphometrically, intimal fibrosis with or without atheroma was more common in subarachnoid arteries in BE than in HH and NT. In addition, the media of the subarachnoid and medullary arteries tended to be thicker in BE than in HH and significantly thicker than in NT. These findings suggest that the duration or severity of hypertension or both have a greater effect on the cerebral arteries in BE than HH. Our heart weight data also seem to support this assumption in that the heart weight of the Japanese patient with BE was 740 g compared with a mean of 420 g for four patients with HH (range 380–460 g).It was reported that BE patients and hypertensive patients with magnetic resonance imaging findings of advanced periventricular hyperintensity lack a definite drop of more than 10 mmHg in their nocturnal systolic blood pressure (“non-dipper”), and that the absolute value of their mean 24-h blood pressures are not always higher than those of patients who do have lower nocturnal systolic blood pressures (“dippers”) [10, 11]. Therefore, not only severe hypertension, but also non-dipper hypertension may predispose to BE. The medullary arteries exposed to severe hypertensive burden will be more prominently damaged than the subarachnoid arteries, because the cerebral medullary artery has a thinner media initially as seen in the NT group. Fukasawa [2] showed in a morphometrical study of cerebral arterial casts of NT human specimens that the physiological drop in blood pressure along the course of the cerebral medullary arteries is larger than that in the arteries of the cortex or striatum, due to their greater length. When such thin-walled arteries are exposed to chronic hypertension, these will adapt to it initially via medial hypertrophy and intimal and/or adventitial fibrosis, but eventually the hypertension will cause segmental destruction and loss of medial SMCs, sometimes with exudation of blood plasma and microaneurysm. Medial hypertrophy itself limits vasodilatation [5]. Additionally, the present study disclosed that many cerebral medullary arteries normally have dilated segments in the intracortical and subcortical regions, which is up to ten times the diameter at the penetrating site of the cortical surface. The tensile force on the artery wall increases in the dilated segment which may also be a mechanism for the preferential involvement of the medullary arteries in BE.

Our morphometrical observations suggest that medial hypertrophy in BE reaches a maximum level in almost every case that has survived without catastrophic events

such as brain hemorrhage or massive infarction. Some cases (case 2, 4 and 6) of HH showed medial hypertrophy of a grade similar to that seen in BE, but the other vascular changes were less severe than in BE. This discrepancy among individuals may be explained by the grade and/or duration of the hypertensive burden. If patients with severe hypertension and non-dipper hypertension survive otherwise fatal hypertensive events, they may progress to BE. However, predispositional differences in tolerance or vulnerability to hypertension or in contractibility of severely hypertrophied cerebral subarachnoid and cortical arteries, which may induce counter-steal of artrial blood flow to medullary arteries [7], may also play a role.

References

1. Fisher CM (1989) Binswanger's encephalopathy: a review. J Neurol 236:65–79
2. Fukasawa H (1969) Hermodynamical studies of cerebral arteries by means of mathematical analysis of arterial casts. Tohoku J Exp Med 99:255–268
3. Furuta A, Ishii N, Nishihara Y, Horie A (1991) Medullary arteries in aging and dementia. Stroke 22:442–446
4. Furuyama M, Torikai T, Suwa N (1962) Histometrical investigations of arteries in reference to arterial hypertension. Tohoku J Exp Med 76:388–414
5. Heistad DD, Mayhan WG, Coyle P, Baumbach GL (1990) Impaired dilatation of cerebral arterioles in chronic hypertension. Blood Vessels 27:258–262
6. Jellinger K, Neumayer E (1964) Progressive subcorticale Vasculäre Encephalopathie Binswanger. Eine klinisch-neuropathologische Studie. Arch Psychiatr Nervenkr 205:523–554
7. Okeda R (1973) Morphometrische Vergleichsuntersuchungen an Hirnarterien bei Binswangerscher Encephalopathie und Hochdruckencephalopathie. Acta Neuropathol (Berl) 26:23–43
8. Olszewski S (1962) Subcortical arterisclerotic encephalopathy. World Neurol 3:359–375
9. Pellissier J-F, Poncet M (1989) Binswanger's encephalopathy. Handb Clin Neurol 54:221–233
10. Shimada K, Kawamoto A, Matsubayashi K, Nishinaga M, Kimura S, Ozawa T (1992) Diurnal blood pressure variations and silent cerebrovascular damage in elderly patients with hypertension. J Hypertens 10:875–878
11. Tohgi H, Chiba K, Kimura M (1991) Twenty-four-hour variation of blood pressure in vascular dementia of the Binswanger type. Stroke 22:603–608